nature cell biology

O_2 regulates stem cells through Wnt/β-catenin signalling

Jolly Mazumdar[1,6,7], W. Timothy O'Brien[2], Randall S. Johnson[3], Joseph C. LaManna[4], Juan C. Chavez[5], Peter S. Klein[2] and M. Celeste Simon[1,6,8]

Stem cells reside in specialized microenvironments or 'niches' that regulate their function. *In vitro* studies using hypoxic culture conditions (< 5% O_2) have revealed strong regulatory links between O_2 availability and functions of stem and precursor cells[1–6]. Although some stem cells are perivascular, others may occupy hypoxic niches and be regulated by O_2 gradients. However, the underlying mechanisms remain unclear. Here, we show that hypoxia inducible factor-1α (HIF-1α), a principal mediator of hypoxic adaptations, modulates Wnt/β-catenin signalling in hypoxic embryonic stem (ES) cells by enhancing β-catenin activation and expression of the downstream effectors LEF-1 and TCF-1. This regulation extends to primary cells, including isolated neural stem cells (NSCs), and is not observed in differentiated cells. *In vivo*, Wnt/β-catenin activity is closely associated with low O_2 regions in the subgranular zone of the hippocampus, a key NSC niche[7]. *Hif-1α* deletion impairs hippocampal Wnt-dependent processes, including NSC proliferation, differentiation and neuronal maturation. This decline correlates with reduced Wnt/β-catenin signalling in the subgranular zone. O_2 availability, therefore, may have a direct role in stem cell regulation through HIF-1α modulation of Wnt/β-catenin signalling.

Activation of the Wnt/β-catenin pathway is characterized by 1) stabilization of cytoplasmic β-catenin after receptor engagement by Wnt ligands; 2) β-catenin nuclear translocation, 3) β-catenin interaction with lymphoid enhancer-binding factor-1/T-cell factor-1 (LEF/TCF) transcription factors; and 4) stimulation of target genes[8,9]. To determine whether this pathway is modulated by O_2 availability, we transiently transfected murine ES cells and P19 embryonal carcinoma (EC) cells with a luciferase-based TOP-Flash (TCF optimal promoter) Wnt reporter plasmid, and compared reporter activity under normoxic (21% O_2) and hypoxic (1.5% O_2) conditions. Exposure to hypoxia significantly enhanced reporter activity (2-fold) in both embryonic cell lines (Fig. 1a; Supplementary Information, Fig. S1a, b). Hypoxic exposure also increased levels of nuclear β-catenin, LEF-1 and TCF-1 proteins (Fig. 1b). Analysis of hypoxic cells by quantitative real-time PCR (qRT–PCR) showed increased expression (2–6-fold) of Wnt target genes, such as *Axin2* and *Dkk-4* (Dickkopf-4), and β-catenin activators, *Lef-1* and *Tcf-1* (Fig. 1c). This is consistent with our previous data showing increased *Lef-1* expression in hypoxic mouse ES cells[10]. HIF-1α protein stabilization and upregulation of the HIF-1α target *Pgk-1* confirmed the induction of a hypoxic response (Fig. 1b, c).

Hypoxia exerted a similar effect in stimulated cells. Wnt pathway stimulators, including 6-bromoindirubin-3′ oxime (BIO) and lithium chloride (LiCl), or Wnt-3a-conditioned medium (Wnt-3a CM), enhanced reporter activity by about 20-fold, whereas exposure to hypoxia increased TOP-Flash activity 50–80-fold in stimulated cells, compared with untreated control cells (Fig. 1d; Supplementary Information, Fig. S2a, b). Exposure to hypoxia also further increased expression of Wnt target genes *Lef-1* and *Dkk-4* in stimulated cells (Fig. 1e). TOP-Flash assays in RNAi-mediated β-catenin-depleted cells confirmed the involvement of β-catenin in hypoxia-induced luciferase activity (Fig. 1f). We excluded the possible involvement of other signalling pathways thought to promote β-catenin stabilization (for example, Akt/PI3K) by showing that after inhibition of glycogen synthase kinase-3β (GSK-3β)[11], GSK-3β phosphorylation levels remained unchanged under hypoxic conditions (Supplementary Information, Fig. S1c). Collectively, these data indicate that ES and P19 EC cells maintain constitutively active Wnt signalling that is β-catenin-dependent, and markedly enhanced by hypoxia.

Hypoxic induction of Wnt signalling was also evident in cell proliferation assays. The number of hypoxic ES cells was increased when compared with normoxic cells (Fig. 1g). Cell survival was also increased, as hypoxic exposure had modest effects on ES cell cycle, but significantly reduced apoptotic cell death (Supplementary Information, Fig. S2c, d). Addition of Wnt-3a CM, which stimulates cell expansion and self-renewal[12], increased the numbers of both normoxic and hypoxic cells, compared with untreated controls. By contrast, treatment with Dickkopf-1 (DKK-1), an extracellular Wnt pathway inhibitor, exclusively decreased the number of hypoxic cells (Fig. 1g). Of note, DKK-1 treatment downregulated TOP-Flash activity in both normoxic and hypoxic ES cells (Fig. 1h), suggesting that hypoxia sensitizes ES cells to the growth effects of Wnt/β-catenin signalling.

[1]Abramson Family Cancer Research Institute,[2] Division of Hematology-Oncology, University of Pennsylvania School of Medicine, Philadelphia, PA 19104, USA. [3]Division of Biological Sciences, U C San Diego, La Jolla, CA 92093, USA. [4]Department of Physiology and Biophysics, Case Western Reserve University, Cleveland, Ohio 44106, USA. [5]Translational Medicine, Wyeth Research, Collegeville, Pennsylvania, PA 19426, USA. [6]Howard Hughes Medical Institute, University of Pennsylvania, Philadelphia, Pennsylvania 19104, USA. [7]Current address: Clinical Biomarkers, Oncology R&D, GlaxoSmithKline, Collegeville, Pennsylvania 19426, USA.
[8]Correspondence should be addressed to M.C.S. (e-mail: celeste2@mail.med.upenn.edu)

Received 28 July 2010; accepted 25 August 2010; published online 19 September 2010; DOI: 10.1038/ncb2102

© 2010 Macmillan Publishers Limited. All rights reserved.

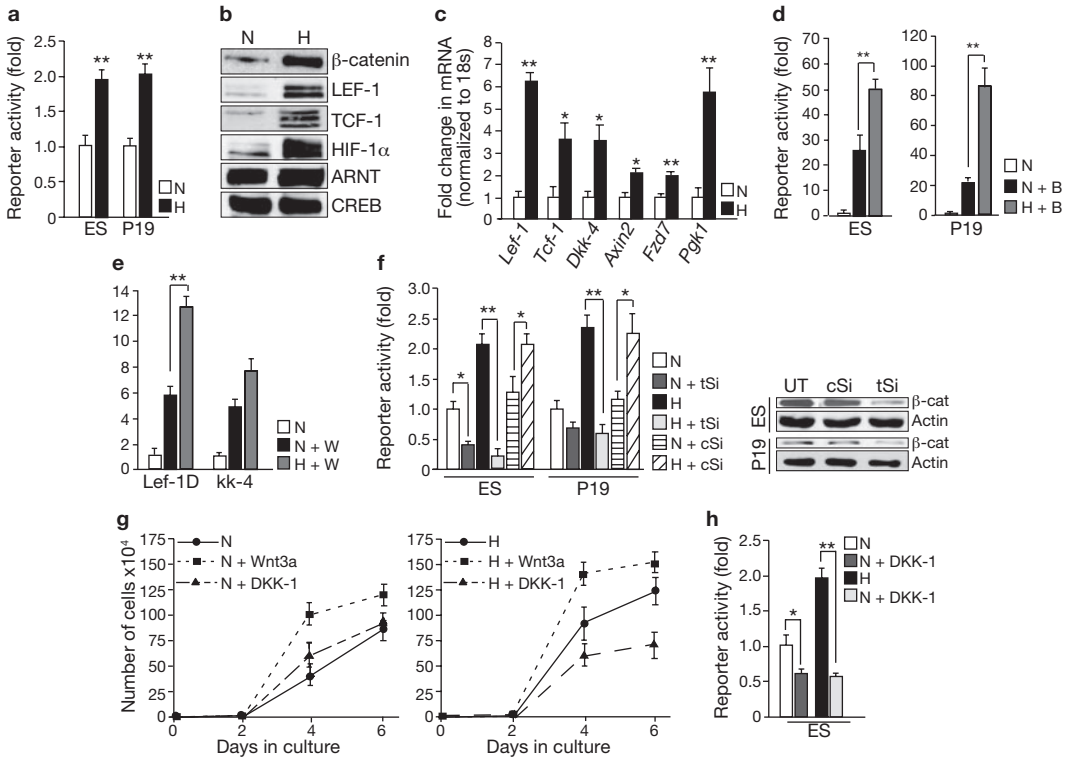

Figure 1 Hypoxia activates Wnt/β-catenin signalling in mouse embryonic cells. (**a**) ES and P19 EC cells transiently transfected with TOP-Flash and pRL-SV40 plasmids were grown under normoxic (N, 21% O_2) or hypoxic (H, 1.5% O_2 for 16h) conditions ($n = 9$). Data indicate luciferase assays, performed using a dual luciferase protocol. (**b**) Western blot analysis of β-catenin and LEF-1/TCF-1 in nuclear extracts from ES cells under O_2 conditions indicated. CREB served as a loading control. (**c**) qRT–PCR analysis of Wnt target gene levels in hypoxic ES cells relative to 18S rRNA levels, normalized to normoxic cells ($n = 9$). (**d**) TOP-Flash activity in ES and P19 EC cells treated with 200 nM bromoindirubin-3′ oxime (B) and cultured either in hypoxic or normoxic conditions ($n = 9$). (**e**) qRT–PCR analysis of Wnt-3a CM-treated ES cells (W) show increased induction of Wnt target genes under hypoxic, compared with normoxic conditions ($n = 6$). (**f**) Marked reduction in reporter activity in ES and P19 EC cells transfected with pools of siRNA against *β-catenin* at the indicated O_2 levels (UT: untransfected, tSi: target siRNA, cSi: control siRNA) ($n = 6$; left panel). Western blot analysis of silenced *β-catenin* 48 h after transfection (right panel). (**g**) Growth rate of ES cells treated with Wnt-3a CM, or the Wnt inhibitor DKK-1 (300 ng ml^{-1}) under the indicated O_2 conditions ($n = 3$). **(h)** TOP-Flash activity in ES cells treated with DKK-1 (300 ng ml^{-1}; $n = 3$). $^*P < 0.05$, $^{**}P < 0.005$., Student's *t*-test (error bars represent s.d.). Uncropped images of blots are shown in Supplementary Information, Fig. S7.

One of the primary mediators of hypoxic responses is HIF-1, a heterodimeric transcription factor containing an O_2-sensitive α subunit (HIF-1α) and a constitutively expressed β subunit (HIF-1β, also known as ARNT). To determine whether hypoxia activates Wnt signalling through HIF-1, we analysed TOP-Flash activity in *Hif-1α*$^{-/-}$ ES cells. In contrast to a report showing HIF-1α-mediated repression of Wnt signalling in colon cancer cells[13], *Hif-1α* deletion significantly downregulated TOP-Flash activity in hypoxic ES cells, but had minimal effect on basal activity (Fig. 2a). Combined treatment of Wnt-3a CM and hypoxia did not superinduce TOP-Flash activity in *Hif-1α*$^{-/-}$ cells (Fig. 2b), and loss of *Hif-1α* had no effect on normoxic responses to Wnt stimulation (Fig. 2b). However, normoxic HIF-1α stabilization in wild-type ES cells by the hypoxia-mimetic deferoxamine significantly restored reporter activity (>1.5-fold; Fig. 2a). We observed a similar regulatory link between hypoxic ARNT activity and Wnt/β-catenin signalling (Fig. 2c). Deletion of *Hif-1α* and *Arnt* also diminished expression of Wnt target genes, including *Dkk-4*, *Lef-1* and *Tcf-1*, under hypoxic conditions (Fig. 2d, e; Supplementary Information, Fig. S3a). Thus, hypoxic induction of Wnt/β-catenin signalling is mediated by HIF-1α/ARNT complexes. Moreover, as expected from increased levels of both β-catenin and LEF-1 in hypoxic cells (Fig. 1b), we detected increased association of nuclear β-catenin, extracted from hypoxic ES cells with immunoprecipitated LEF-1 (Fig. 2f). Intriguingly, we noted reduced levels of β-catenin in whole-cell extracts of hypoxic *Hif-1α*$^{-/-}$ cells, compared with hypoxic *Hif-1α*$^{+/+}$ (Fig. 2e).

As hypoxic induction of *Lef-1* and *Tcf-1* mRNA and corresponding proteins strongly correlated with HIF-1α protein accumulation, we examined whether HIF-1α contributes directly to increased transcription of *Lef/Tcf* genes. Analysis of murine *Lef-1* and *Tcf-1* gene sequences revealed multiple putative HREs (hypoxia response elements) spanning exon 1 and the upstream promoter and enhancer regions (+3000 bp; Fig. 2g). In chromatin immunoprecipitation (ChIP) assays, HIF-1α association at each genomic region tested was 4–10-fold greater in hypoxic ES cells than in normoxic cells (Fig. 2g). HIF-1α, therefore, regulates LEF-1/TCF-1 protein abundance and function in embryonic cells. In proliferation assays, neither *Hif-1α*$^{-/-}$ nor *Arnt*$^{-/-}$ cells showed a growth advantage under hypoxic conditions when compared with the corresponding wild-type *Hif-1α*$^{+/+}$ and *Arnt*$^{+/+}$ cells (Supplementary Information, Fig. S3b, c).

Stem and committed progenitor cells can respond differently to low O_2 signals[5]. We therefore examined whether hypoxic effects on Wnt/β-catenin signalling are a function of differentiation stage. Embryonic cells were stimulated with neuronal supplements (N2B27) to form neuronal precursors[14]. Thereafter, we subjected ES and P19 EC cell-derived

© 2010 Macmillan Publishers Limited. All rights reserved.

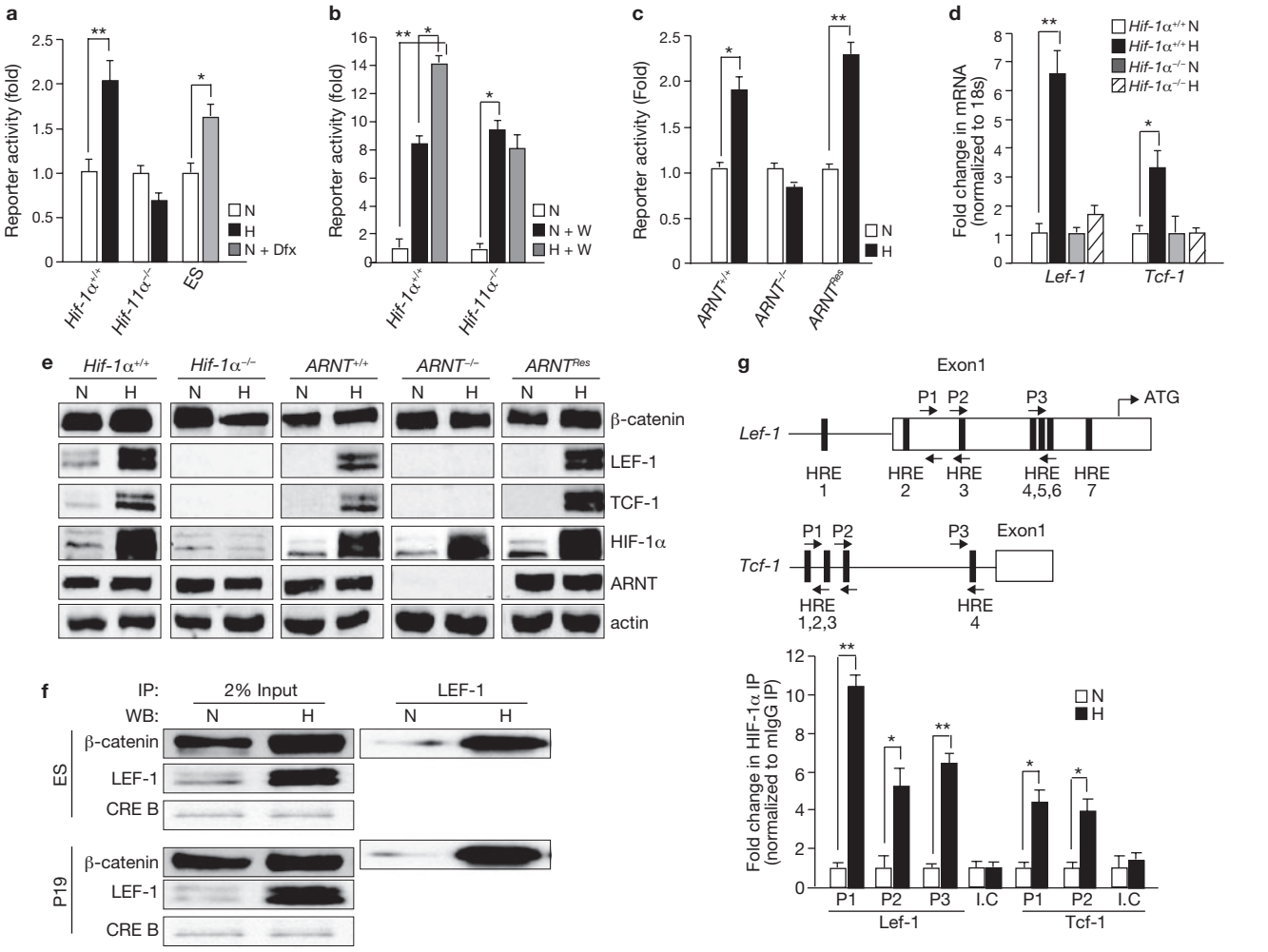

Figure 2 HIF-1 (HIF-1α/ARNT complex) mediates hypoxia-induced Wnt signalling in embryonic cells. (**a**) Compared with hypoxic *Hif-1α*$^{+/+}$ cells (left panel), *Hif-1α*$^{-/-}$ ES cells (middle panel) show attenuated TOP-Flash activity under hypoxic conditions. Reporter activity was increased in normoxic ES cells treated with DFX for 16 h ($n = 9$; right panel). (**b**) TOP-Flash activity in *Hif-1α*$^{+/+}$ and *Hif-1α*$^{-/-}$ cells stimulated with Wnt-3a CM (W) and cultured under the indicated O_2 conditions ($n = 9$). (**c**) TOP-Flash activity is attenuated in hypoxic *Arnt*$^{-/-}$ ES cells, compared with hypoxic *Arnt*$^{+/+}$ cells ($n = 9$), and rescued in hypoxic *Arnt*^{Res} cells (*Arnt*$^{-/-}$ cells with restored *Arnt* expression). (**d**) qRT–PCR analysis of *Hif-1α*$^{-/-}$ cell extracts for Wnt target gene expression ($n = 6$). (**e**) Western blot analysis of β-catenin, LEF-1 and TCF-1 proteins in whole-cell extracts of null cells (indicated by the absence of specific protein) or corresponding wild-type cells cultured either under normoxic or hypoxic conditions. Actin served as the loading control. (**f**) Immunoprecipitation with LEF-1 antibody was performed on nuclear extracts of normoxic or hypoxic ES cells. CREB served as the loading control. (**g**) ES cells were cultured under 21% or 1.5% O_2 for 16 h and then assayed by ChIP. After immunoprecipitation with antibodies against HIF-1α or isotype control, DNA extracts were assessed by qRT–PCR. The results of each genomic region tested (upper panel) are expressed as fold difference between HIF-1α IP and mouse IgG control (lower panel). *Lef-1* coding region (I.C) served as a control. Data shown are mean ± s.d. ($n = 4$; $^*P < 0.05$, $^{**}P < 0.005$., Student's *t*-test and one-way ANOVA (**a**–**d**, **g**). Uncropped images of blots are shown in Supplementary Information, Fig. S7.

neurons expressing the neuronal markers β-tubulin III (β-tubIII) and doublecortin (DCX) (Fig. 3a; Supplementary Information, Fig. S4a) to TOP-Flash assays. The transfection efficiency was monitored using GFP as a reporter (data not shown). Whereas hypoxia enhanced TOP-Flash activity in undifferentiated ES and P19 cells (Fig. 3b), it did not have any effect on the embryonic cell- derived neurons. This observation suggests that hypoxia selectively activates Wnt/β-catenin signalling in undifferentiated cells. We also observed hypoxic induction of *Lef-1* and *Tcf-1* genes exclusively in undifferentiated cells (Fig. 3c). Furthermore, neuronal differentiation coincided with a significant loss of baseline *Lef-1*/*Tcf-1* levels (3–5-fold; Fig. 3c). We suggest that the *Lef-1* and *Tcf-1* loci become epigenetically modified and therefore inaccessible to HIF-1 in differentiated cells.

It has been shown that LEF/TCF overexpression increases β-catenin nuclear translocation, and activates transcription in various embryonic cell types[15,16]. To investigate whether β-catenin accumulation in hypoxic ES cells involved *Lef-1* induction, we engineered LEF-1-overexpressing ES cells (ES-*Lef-1*). LEF-1 overexpression resulted in increased levels of nuclear β-catenin under normoxic conditions relative to vector controls (Fig. 3d). Also, ES-*Lef-1* cells showed enhanced cell proliferation, and were sensitive to DKK-1 inhibition (Supplementary Information, Fig. S4c). This observation recapitulated Wnt/β-catenin-dependent hypoxic effects on ES cell proliferation (Fig. 1g). Moreover, we reproduced nuclear β-catenin–HIF-1α interaction in hypoxic ES cells (see Supplementary Information, Fig. S4b), similarly to previous observations in differentiated neoplastic cells[13], further highlighting the

© 2010 Macmillan Publishers Limited. All rights reserved.

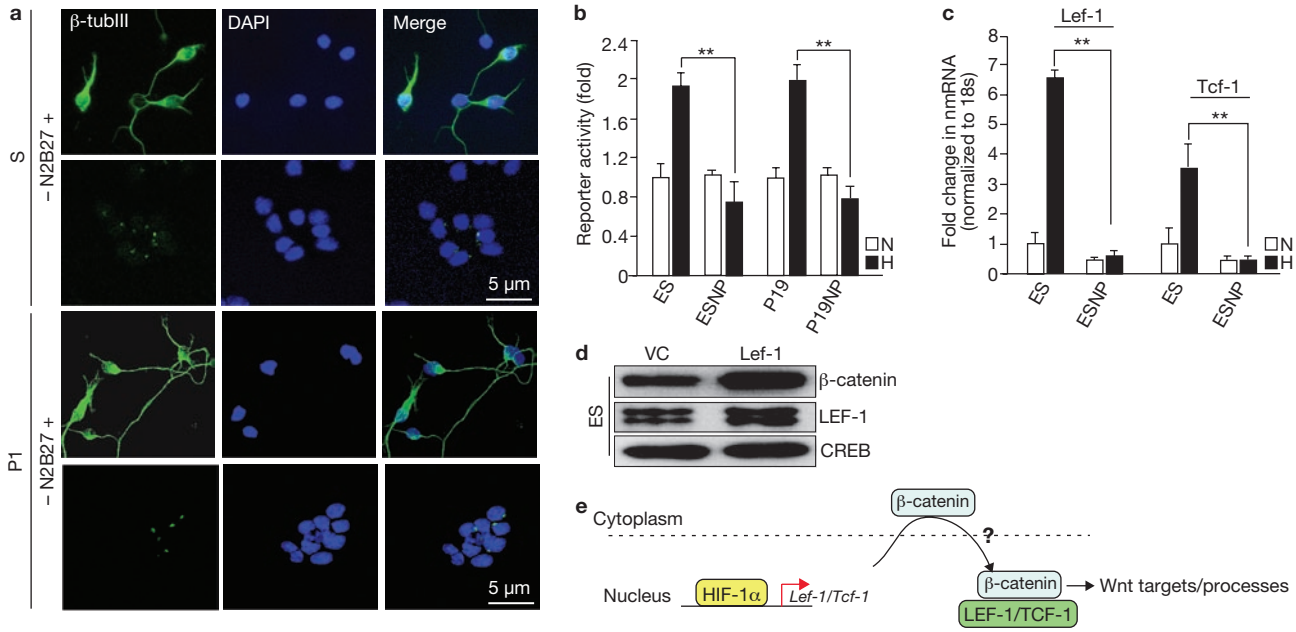

Figure 3 O_2 regulation of Wnt/β-catenin signalling is differentiation-stage specific. (**a**) ES and P19 EC cells were treated with (+) or without (–) N2B27 neuronal growth and differentiation supplements, and monitored for the formation of neuronal progenitors (NP) through the expression of neuronal marker β-tub III. (**b**) Compared with hypoxic undifferentiated controls, ES and P19 EC cell-derived NPs demonstrate attenuated TOP-Flash reporter activity under hypoxic conditions ($n = 3$) (**c**) NPs derived from ES cells were cultured under normoxic or hypoxic conditions for 16 h and assessed for *Lef/Tcf* gene expression by qRT–PCR. Data shown in **b** and **c** are mean ± s.d. ($n = 3$; $^{**}P < 0.005$., Student's *t*-test). (**d**) Western blot analysis of nuclear extracts of ES-*Lef-1* and the corresponding control virus-transduced ES cells (VC) cultured under normoxic conditions. CREB served as the loading control. (**e**) Schematic representation of a model wherein hypoxia (via HIF-1α) induces β-catenin transcriptional effectors, *Lef-1* and *Tcf-1*, resulting in increased nuclear translocation of β-catenin (? indicates mechanism is unknown), subsequent interaction between β-catenin and LEF-1/TCF-1 and activation of Wnt target genes. Scale bars, 5 μm. Uncropped images of blots are shown in Supplementary Information, Fig. S7.

involvement of LEF-1 in differentiation-stage-specific responses of the Wnt/β-catenin pathway to hypoxia. Taken together, we propose a model where HIF-1α regulates *Lef-1* and *Tcf-1* in undifferentiated cells, leading to increased nuclear β-catenin–LEF/TCF interaction, and activation of Wnt/β-catenin targets (Fig. 3e).

To determine the physiological relevance of the model described above, we next investigated whether decreased O_2 levels correlate with Wnt/β-catenin activity *in vivo*. We screened for areas of Wnt/β-catenin activity in a Wnt reporter (*BAT–GAL*) mouse strain, using β-galactosidase immunostaining[17]. We compared its distribution with that of low O_2 regions detected by immunostaining with the hypoxia marker pimonidazole hydrochloride. Pimonidazole detects O_2 partial pressures of less than 10 mm Hg (~1.3% O_2)[18]. Active Wnt/β-catenin signalling was detected in close proximity to low O_2 regions in both embryonic and adult brain (Fig. 4a, b; Supplementary Information, Fig. S5a–d). One such region positive for Wnt/β-catenin activity was the subgranular zone of the dentate gyrus (Fig. 4a; Supplementary Information, Fig. S5e–g), a primary neurogenic niche in which adult hippocampal progenitors (AHPs) proliferate and differentiate into dentate granule neurons[7]. Pimonidazole clearly marked the subgranular zone, as identified by its colocalization with the NSC marker Sox2 (Fig. 4c, d). Importantly, enumeration of blood vessels marked by laminin immunostaining revealed a much higher ratio of nuclei to blood vessels within the granule cell layer of the dentate gyrus, compared with other areas in the brain, including the adjacent hippocampal Oriens layer, and the cerebellar granule cell layer (Fig. 4e–g). Other vascular markers such as CD31 and India ink showed a similar trend (Supplementary Information, Fig. S5h–k). This suggests that hypoxia within the dentate gyrus, as independently confirmed by HIF-1α stabilization and the expression of hypoxia responsive genes carbonic anhydrase IX (CAIX) and vascular endothelial growth factor (VEGF), (Supplementary Information, Fig. S5l–q), is probably a consequence of O_2 limitation, attributable to fewer blood vessels being present.

To further examine the potential link between HIF-1α and Wnt/β-catenin signalling *in vivo*, we engineered a *BAT–GAL* reporter line in the background of conditional global HIF-1α mutants (g*Hif-1α*$^{\Delta/\Delta}$, *BAT-GAL*^{Tg}). Because global *Hif-1α* deletion results in embryonic lethality[19], we crossed mice homozygous for the *loxP*-flanked (floxed) *Hif-1α* allele (*Hif-1α*$^{f/f}$) with *Hif-1α*$^{f/f}$ mice expressing tamoxifen-inducible Cre driven by a ubiquitin C (*UbC*) promoter, such that tamoxifen administration would result in global postnatal *Hif-1α* (g*Hif-1α*$^{\Delta/\Delta}$) deletion (Supplementary Information, Fig. S6a, b). *Hif-1α* deletion reduced hippocampal Wnt signalling, as shown by loss of *BAT–GAL* reporter activity in mice expressing the *BAT–GAL* transgene ($n = 3$; Fig. 4h, i; Supplementary Information, Fig. S6c, d). *Hif-1α* deletion also decreased expression of Wnt target genes such as *Dkk-4* (undetected), *Lef-1* and *Axin2* (2.5-fold; $n = 5$) in g*Hif-1α*$^{\Delta/\Delta}$ animals (Fig. 4j).

We used the subgranular zone as a model stem cell niche, to evaluate the role of HIF-1α in stem cell functions, because Wnt/β-catenin signalling has been identified as a positive regulator of neurogenesis in the subgranular zone of adult hippocampus[7]. On the basis of the subgranular zone HIF-1α -Wnt /β-catenin connection, we hypothesized that loss of HIF-1α may result in aberrant neurogenesis *in vivo*. We analysed the dentate gyrus of young adult (7–8 weeks) g*Hif-1α*$^{\Delta/\Delta}$ mice or control mice

© 2010 Macmillan Publishers Limited. All rights reserved.

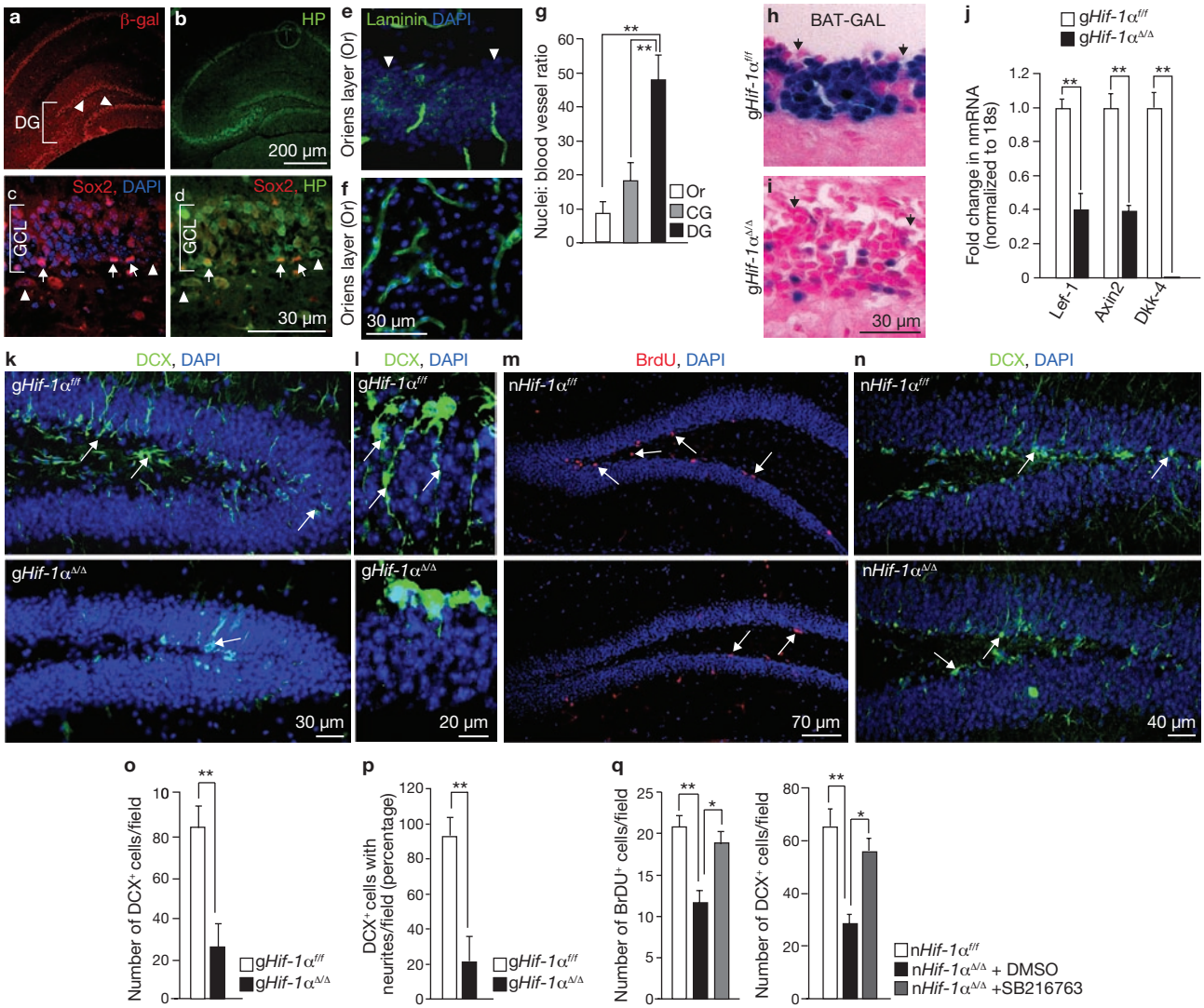

Figure 4 Deletion of *Hif-1α in vivo* suppresses adult hippocampal neurogenesis. (**a**) Wnt activity in the adult dentate gyrus (DG) is marked by β-galactosidase (β-gal) immunostaining (red) in *BAT–GAL* reporter mice. Arrowheads indicate the subgranular zone (SGZ) in the DG. (**b**) Hypoxic regions within the adult hippocampus marked by pimonidazole staining (HP, green) include the adult DG. (**c**) The subgranular zone of the DG is marked by the stem cell marker Sox2. (**d**) Colocalization of pimonidzole with Sox2$^+$ cells indicates a hypoxic subgranular zone. Arrowheads (**c, d**) indicate the orientation of the subgranular zone of the granule cell layer (GCL). (**e**, **f**) Laminin staining marks blood vessels in the DG (**e**), and in the adjacent hippocampal Oriens layer (Or) (**f**). (**g**) Quantification of the nuclei: blood vessel ratio in the DG, Or and cerebellar granule layer (CG). Data shown are mean ± s.e.m. ($n = 3$; 5 sections per animal, $^{**}P < 0.005$, Student's *t*-test). (**h**, **i**) X-gal staining of the DG of *Hif-1α*$^{f/f}$, *BAT–GAL*^{Tg} (**h**) and g*Hif-1α*$^{Δ/Δ}$, *BAT–GAL*^{Tg} (**i**) animals ($n = 3$; 5 sections per animal). (**j**) qRT–PCR analysis of hippocampal extracts for Wnt target genes (Lef-1, Axin2 and Dkk4; g*Hif-1α*$^{f/f}$, $n = 3$ and g*Hif-1α*$^{Δ/Δ}$, $n = 5$). (**k, o**) Significant reduction of DCX$^+$ cells (arrows) in g*Hif-1α*$^{Δ/Δ}$ subgranular zone and GCL, compared with control *Hif-1α*$^{f/f}$ animals ($n = 7$). (**l, p**) There were significantly fewer DCX$^+$ cells with neurites in g*Hif-1α*$^{Δ/Δ}$ DG, as compared with g*Hif-1α*$^{f/f}$ DG. DCX$^+$ cells with processes greater than 20 μM were counted as positive for neurites ($n = 7$). (**m, n, q**) Lack of neuronal *Hif-1α* in the subgranular zone reduces NSC proliferation (**m, q** left panel), as indicated by BrdU$^+$ cells (arrows;, and NSC differentiation (**n, q** right panel), as indicated by DCX$^+$ cells (arrows) indicate DCX$^+$ cells with neuritis; arrowheads indicate the direction of subgranular zone ($n = 6$). (**q**) Quantification of BrdU$^+$ and DCX$^+$ cells in *nHif-1α*$^{Δ/Δ}$ DG treated with SB216763 (2 mg kg^{-1}) every other day for 2 weeks. Vehicle-treated *nHif-1α*$^{Δ/Δ}$ and untreated *nHif-1α*$^{f/f}$ mice served as controls. Data shown are mean ± s.e.m. ($n = 6$; $^*P < 0.05$, $^{**}P < 0.005$., Student's *t*-test (**j, o, p**) and one-way ANOVA (**q**). Scale bars: **b**, 200 μm; **d**, 30 μm; **f**, 30 μm; **h**, 30 μm; **k**, 30 μm, **l**, 20 μm; **m**, 70 μm; **n**, 40 μm.

lacking Cre (g*Hif-1α*$^{f/f}$) for cells expressing the early neuronal marker doublecortin (DCX). g*Hif-1α*$^{Δ/Δ}$ dentate gyrus showed a 3.4-fold reduction in DCX$^+$ cells, compared with g*Hif-1α*$^{f/f}$ control animals ($n = 7$; Fig. 4k, o). Furthermore, the capacity of DCX$^+$ neurons in the g*Hif-1α*$^{Δ/Δ}$ mice to form neurites was markedly reduced (4-fold; $n = 7$; Fig. 4l, p), a phenotype critical for integration of the newborn neurons into the existing neuronal circuitry.

To distinguish between cell-intrinsic versus cell-extrinsic effects underlying the effect of HIF-1α on hippocampal neurogenesis, we further analysed adult neurogenesis in a neuron-specific *Hif-1α* deletion model. To selectively delete HIF-1α from mouse neurons, we crossed *Hif-1α*$^{f/f}$ mice with R1ag no.5 (R1) mice expressing Cre driven by the calcium/calmodulin-dependent kinase (αCamKII) promoter[20,21]. Cre expression in the R1 animals results in postnatal neuronal *Hif-1α*

© 2010 Macmillan Publishers Limited. All rights reserved.

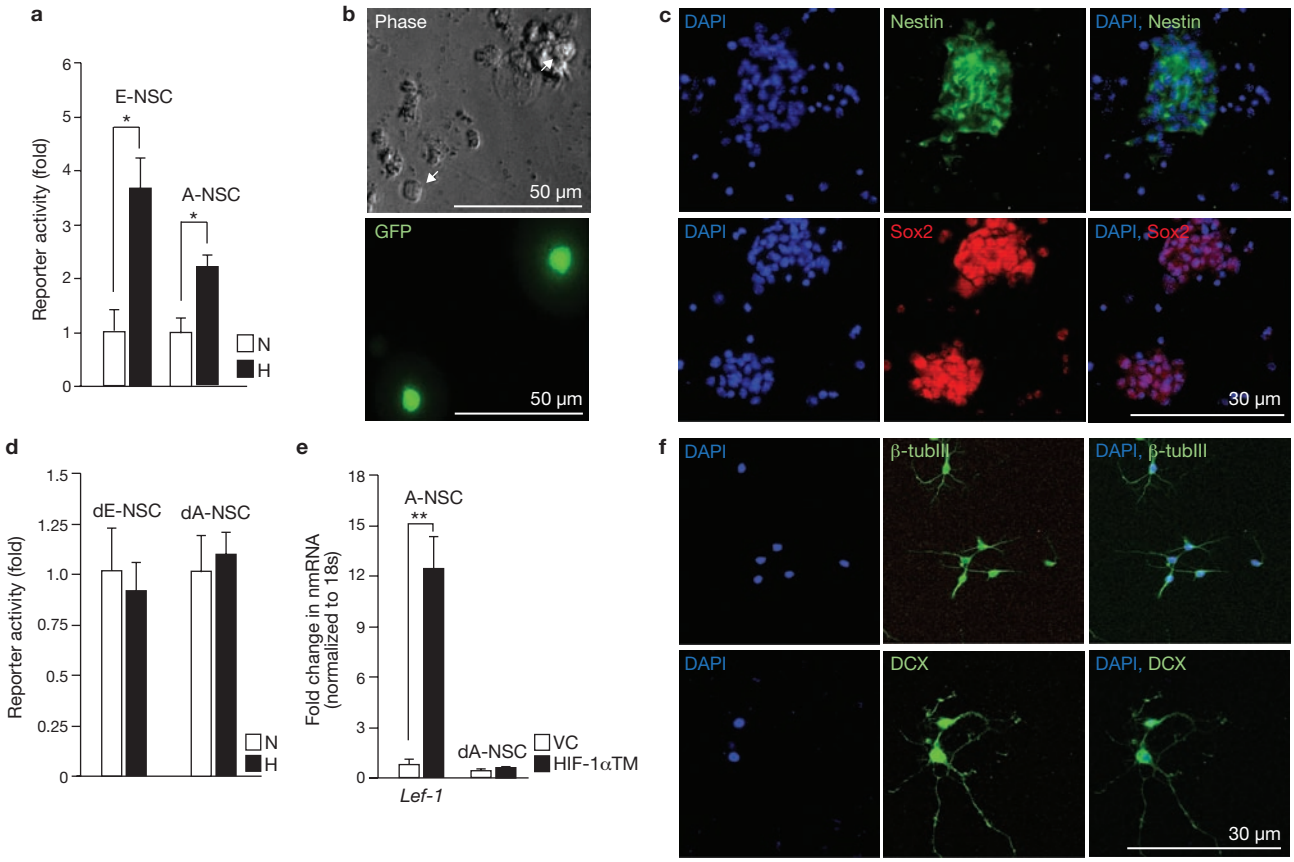

Figure 5 Neuronal *Hif-1α* regulates neurogenesis through Wnt/β-catenin signalling. (**a**) E14 NSCs (E-NSC) or adult NSCs (A-NSC) isolated from the hippocampus of mice aged 4–6 weeks were cultured as neurospheres, and used for TOP-Flash assay under normoxic or hypoxic conditions ($n = 6$). (**b**) Transfection efficiency for NSC TOP-Flash assays was monitored with GFP in 2-day post-dissociation neurospheres (white arrows in phase). (**c**) Neurospheres were assayed for progenitor markers including Nestin (upper panel) and Sox2 (lower panel). (**d**) TOP-Flash assay in differentiated E14 embryonic (dE-NSC), or adult NSCs (dA-NSC) cultured under normoxic or hypoxic conditions ($n = 6$). (**e**) qRT–PCR analysis of *Lef-1* levels in A-NSCs or differentiated A-NSCs (dA-NSC) transfected with HIF-1α TM plasmid or corresponding vector control (VC; $n = 3$). (**f**) Differentiation of neurospheres was assessed by the expression of differentiation markers including β-tubIII (upper panel) and DCX (lower panel). Data shown are mean ± s.d.; $*P < 0.05$, $**P < 0.005$., Student's *t*-test (**a**, **d**, **e**). Scale bars: **b**, 50 μm; **c**, 30 μm; **f**, 30 μm.

(*nHif-1α*$^{\Delta/\Delta}$) deletion in the forebrain[21], including Sox2$^+$ cells in the subgranular zone of the dentate gyrus (Supplementary Information, Fig. S5r–t). Similarly to global *Hif-1α* deletion, neuronal *Hif-1α* loss significantly reduced the number of BrdU$^+$ (which labels proliferating NSCs and progenitors) cell (2.2-fold) and DCX$^+$ newborn neurons (2-fold) in the subgranular zone of *nHif-1α* $^{\Delta/\Delta}$ mice as compared with *nHif-1α*$^{f/f}$ control animals ($n = 6$; Fig. 4m, n, q). Double-immunostaining with BrdU and DCX confirmed that DCX$^+$ cells were derived from NSCs and AHPs (Supplementary Information, Fig. S6e). Moreover, similarly to g*Hif-1α*$^{\Delta/\Delta}$ DCX$^+$ cells, the capacity of DCX$^+$ cells from *nHif-1α*$^{\Delta/\Delta}$ mice to form neurites was markedly reduced (3-fold; $n = 3$; Supplementary Information, Fig. S6f, g). Importantly, the neurogenesis defects were rescued pharmacologically in *nHif-1α*$^{\Delta/\Delta}$ mice treated with GSK-3 inhibitor SB 216763 (2 mg Kg^{-1}), but not in vehicle-treated *nHif-1α*$^{\Delta/\Delta}$ mice ($n = 6$; Fig. 4q). We also made similar observations in *nHif-1α*$^{\Delta/\Delta}$ mice transduced with lentiviruses expressing a constitutively active form of β-catenin (Δ-GSK–β-catenin)[22] ($n = 3$–5 per group; Supplementary Information, Fig. S6h, i). These models cannot exclude a potential role for HIF-1α in regulating trophic signals provided by the post-mitotic mature granule neurons of the dentate gyrus in the survival and integration of NSCs into hippocampal circuitry. Nevertheless, HIF-1α clearly regulates adult neurogenesis by promoting NSC/progenitor cell proliferation and differentiation through Wnt/β-catenin signalling.

We also observed that hypoxic regulation of Wnt/β-catenin activity shown by ES cells is shared by primary cells of the nervous system. Isolated embryonic and adult neural stem cells (E-NSC and A-NSC) transfected with TOP-Flash plasmid showed significantly increased reporter activity under hypoxic conditions (Fig. 5a–c), and this effect was lost in differentiated neurospheres (Fig. 5d, f). Of note, transient transfection with a normoxia-active HIF-1α triple mutant (HIF-1α TM[P402A/P577A/N815A]) plasmid[23] increased *Lef-1* levels by about 12-fold exclusively in the undifferentiated neurospheres (Fig. 5e). Moreover, differentiated neursopheres showed significantly reduced baseline *Lef-1* levels as compared with undifferentiated control neurospheres (Fig. 5e), reminiscent of reduced basal *Lef-1* expression observed in ES cell-derived neurons (Fig. 3c). We conclude that the regulation of Wnt/β-catenin by HIF-1α through *Lef-1* induction represents an important mechanism of stem cell homeostasis, and may be applicable to stem cell microenvironments beyond the hippocampal neurogenic niche.

Numerous adult stem cells have been found closely associated with the vasculature[24–27]. Interestingly, we now demonstrate that low O_2 levels may also contribute to stem cell microenvironments. This suggests that

© 2010 Macmillan Publishers Limited. All rights reserved.

although some adult stem cells occupy well-oxygenated perivascular domains, others reside within hypoxic niches and are regulated by O_2 deprivation. Induction of Wnt/β-catenin signalling by HIF-1α represents a molecular mechanism underlying this regulation. These studies extend the positive effects of HIFs previously shown for other stem cell pathways, including Oct-4 and Notch-1 (refs 28, 29). The opposite result was reported for HCT116 colon cancer cells, in which HIF-1α inhibited Wnt/β-catenin activity[13], suggesting that the interaction between HIF-1α andWnt/β-catenin in undifferentiated stem/ progenitor cells and more differentiated cell types (including neoplastic cells) is functionally distinct. In summary, the present findings confirm the emerging concept that HIFs not only act in metabolic adaptations, but can also regulate critical stem cell phenotypes. □

METHODS

Methods and any associated references are available in the online version of the paper at http://www.nature.com/naturecellbiology/

Note: Supplementary Information is available on the Nature Cell Biology website.

ACKNOWLEDGEMENTS

We thank K. Kinzler and B. Vogelstein for the Wnt (TOP/FOP) reporter constructs; P. Carmeliet for *Hif-1α*$^{-/-}$ ES cells; and E. Brown for *Ubc-Cre-ER*^{T2} mice. We thank X. Sun, Case Western Reserve University, and H. Yu, University of Pennsylvania for technical assistance with tissue harvesting and sectioning. We thank B. Keith and the Simon lab for discussion and critical review of the manuscript. This work was supported by funds from the Howard Hughes Medical Institute (HHMI), the Abramson Family Cancer Research Institute, and the National Institutes of Health (Grant No. MH58324 to P.S.K). M.C.S. is an investigator of the HHMI.

AUTHOR CONTRIBUTIONS

J.M. and W.T.O. designed, performed and analysed the experiments; P.S.K and M.C.S assisted in the interpretation of results; J.C.C. and J.C.L. provided the α*CamKII-Cre- Hif-1α*$^{f/f}$ mice; R.S.J. provided the *Hif-1α*$^{f/f}$ mice; J.M. made the figures and wrote the paper; M.C.S. edited the paper.

COMPETING FINANCIAL INTERESTS

The authors declare that they have no competing financial interests.

Published online at http://www.nature.com/naturecellbiology/Reprints and permissions information is available online at http://npg.nature.com/reprintsandpermissions/

1. Studer, L. *et al.* Enhanced proliferation, survival, and dopaminergic differentiation of CNS precursors in lowered oxygen. *J. Neurosci.* **20,** 7377–7383 (2000).
2. Adelman, D. M., Gertsenstein, M., Nagy, A., Simon, M. C. & Maltepe, E. Placental cell fates are regulated *in vivo* by HIF-mediated hypoxia responses. *Genes Dev.* **14,** 3191–3203 (2000).
3. Genbacev, O., Zhou, Y., Ludlow, J. W. & Fisher, S. J. Regulation of human placental development by oxygen tension. *Science* **277,** 1669–1672 (1997).
4. Adelman, D. M., Maltepe, E. & Simon, M. C. Multilineage embryonic hematopoiesis requires hypoxic ARNT activity. *Genes Dev.* **13,** 2478–2483 (1999).
5. Danet, G. H., Pan, Y., Luongo, J. L., Bonnet, D. A. & Simon, M. C. Expansion of human SCID-repopulating cells under hypoxic conditions. *J. Clin. Invest.* **112,** 126–135 (2003).
6. Morrison, S. J. *et al.* Culture in reduced levels of oxygen promotes clonogenic sympathoadrenal differentiation by isolated neural crest stem cells. *J. Neurosci.* **20,** 7370–7376 (2000).
7. Lie, D. C. *et al.* Wnt signalling regulates adult hippocampal neurogenesis. *Nature* **437,** 1370–1375 (2005).
8. Reya, T. & Clevers, H. Wnt signalling in stem cells and cancer. *Nature* **434,** 843–850 (2005).
9. van de Wetering, M. *et al.* Armadillo coactivates transcription driven by the product of the *Drosophila* segment polarity gene dTCF. *Cell* **88,** 789–799 (1997).
10. Hu, C. J. *et al.* Differential regulation of the transcriptional activities of hypoxia-inducible factor 1 α (HIF-1α) and HIF-2α in stem cells. *Mol. Cell Biol.* **26,** 3514–3526 (2006).
11. Naito, A. T. *et al.* Phosphatidylinositol 3-kinase-Akt pathway plays a critical role in early cardiomyogenesis by regulating canonical Wnt signaling. *Circ. Res.* **97,** 144–151 (2005).
12. Reya, T. *et al.* A role for Wnt signalling in self-renewal of haematopoietic stem cells. *Nature* **423,** 409–414 (2003).
13. Kaidi, A., Williams, A. C. & Paraskeva, C. Interaction between β-catenin and HIF-1 promotes cellular adaptation to hypoxia. *Nat. Cell Biol.* **9,** 210–217 (2007).
14. Ying, Q. L., Stavridis, M., Griffiths, D., Li, M. & Smith, A. Conversion of embryonic stem cells into neuroectodermal precursors in adherent monoculture. *Nat. Biotechnol.* **21,** 183–186 (2003).
15. Huber, O. *et al.* Nuclear localization of β-catenin by interaction with transcription factor LEF-1. *Mech. Dev.* **59,** 3–10 (1996).
16. Molenaar, M. *et al.* XTcf-3 transcription factor mediates β-catenin-induced axis formation in *Xenopus* embryos. *Cell* **86,** 391–399 (1996).
17. Maretto, S. *et al.* Mapping Wnt/β-catenin signaling during mouse development and in colorectal tumors. *Proc. Natl Acad. Sci. USA* **100,** 3299–3304 (2003).
18. Raleigh, J. A. *et al.* Hypoxia and vascular endothelial growth factor expression in human squamous cell carcinomas using pimonidazole as a hypoxia marker. *Cancer Res.* **58,** 3765–3768 (1998).
19. Ryan, H. E., Lo, J. & Johnson, R. S. HIF-1 α is required for solid tumor formation and embryonic vascularization. *EMBO J.* **17,** 3005–3015 (1998).
20. Dragatsis, I. & Zeitlin, S. CaMKIIα–Cre transgene expression and recombination patterns in the mouse brain. *Genesis* **26,** 133–135 (2000).
21. Baranova, O. *et al.* Neuron-specific inactivation of the hypoxia inducible factor 1 alpha increases brain injury in a mouse model of transient focal cerebral ischemia. *J. Neurosci.* **27,** 6320–6332 (2007).
22. Barth, A. I., Stewart, D. B. & Nelson, W. J. T cell factor-activated transcription is not sufficient to induce anchorage-independent growth of epithelial cells expressing mutant β-catenin. *Proc. Natl Acad. Sci. USA* **96,** 4947–4952 (1999).
23. Hu, C. J., Sataur, A., Wang, L., Chen, H. & Simon, M. C. The N-terminal transactivation domain confers target gene specificity of hypoxia-inducible factors HIF-1α and HIF-2α. *Mol. Biol. Cell* **18,** 4528–4542 (2007).
24. Kiel, M. J., Yilmaz, O. H., Iwashita, T., Terhorst, C. & Morrison, S. J. SLAM family receptors distinguish hematopoietic stem and progenitor cells and reveal endothelial niches for stem cells. *Cell* **121,** 1109–1121 (2005).
25. Yoshida, S., Sukeno, M. & Nabeshima, Y. A vasculature-associated niche for undifferentiated spermatogonia in the mouse testis. *Science* **317,** 1722–1726 (2007).
26. Tavazoie, M. *et al.* A specialized vascular niche for adult neural stem cells. *Cell Stem Cell* **3,** 279–288 (2008).
27. Shen, Q. *et al.* Adult SVZ stem cells lie in a vascular niche: a quantitative analysis of niche cell–cell interactions. *Cell Stem Cell* **3,** 289–300 (2008).
28. Covello, K. L. *et al.* HIF-2α regulates Oct-4: effects of hypoxia on stem cell function, embryonic development, and tumor growth. *Genes Dev.* **20,** 557–570 (2006).
29. Gustafsson, M. V. *et al.* Hypoxia requires notch signaling to maintain the undifferentiated cell state. *Dev. Cell* **9,** 617–628 (2005).

© 2010 Macmillan Publishers Limited. All rights reserved.

DOI: 10.1038/ncb2102

METHODS

Cell culture and treatments. *Arnt* $^{-/-}$, *Arnt* ^{Res} and corresponding wild-type (*Arnt*$^{+/+}$) ES cells have been described previously[30,31]. ES cells were cultured as described previously[4]. P19 EC cells (ATCC) were cultured as per the manufacturer's protocol. Hypoxia (0.5%, 1.5% and 3% O_2) was achieved using a HERAcell 240 hypoxic workstation with O_2 control. Deferoxamine (DFX; Calbiochem) was used as a hypoxia-mimetic at a final concentration of 200 μM for 16 h. Wnt-3a conditioned medium (Wnt-3a CM) and corresponding control medium were collected from L Wnt-3A and L cells, respectively (ATCC). LiCl (20 mM, final concentration) and BIO (200 nM, final concentration) were purchased from Sigma.

Reporter assay. Transient transfections of cells with TOP-Flash or FOP-Flash plasmids were performed with Lipofectamine 2000 (Invitrogen) in 24-well plates. Luciferase assays were performed using the dual luciferase protocol (Promega) with the following modification for siRNA: cells were first transfected with siRNA against *β-catenin* (ON-TARGET plus SMART pool L-040628-00-0005, Dharmacon), and after 24 h were co-transfected with firefly (200 ng) and *Renilla* luciferase (20 ng) reporter gene expression plasmids. β-catenin knockdown was verified 48–72 h after transfection by standard western blot procedures.

Apoptosis and cell proliferation. For apoptosis studies, undifferentiated ES monolayers were grown on gelatin-coated coverslips, and cultured under hypoxic conditions for the indicated time period. TUNEL$^+$ cells were visualized using an ApopTag kit (Millipore). TUNEL$^+$ cells were enumerated as a percentage of total number of cells in the field detected by DAPI nuclear staining. Three randomly chosen fields per plate ($n = 3$) were analysed and the mean for each condition calculated. For proliferation analysis, 10^4 cells were seeded on 6 cm^2 plates, and two plates per time point were counted in a haemocytometer over 6 days. Recombinant mouse DKK-1 (R&D systems) was used at a final concentration of 300 ng ml^{-1}. For cell-cycle analysis, ES monolayers were cultured either under normoxic or hypoxic conditions, briefly pulsed with 5′-bromo-2′ 3′-deoxyuridine (BrdU; 10 μm for 20 min), stained with propidium iodide (PI) and analysed by flow cytometry.

qRT-PCR analyses. Total RNA (2 μg of each sample isolated using RNeasy; Qiagen) was reverse transcribed using high capacity cDNA reverse transcription kit (ABI) and assayed for gene expression by SYBR-GREEN technology (ABI). The following primer sequences were used: Lef-1F, 5′-TCCTGAAATCCCCACCTTCT-3′, Lef-1R: 5′-TGGGATAAACAGGCTGACCT-3′; Tcf-1/7F, 5′-CAGCTCCCCCATACTGTGAG-3′; Tcf-1/7R, 5′-TGCTGTCTATATCCGCAGGAA-3′; Dkk-4F, 5′-ACGAAGAAATCACAAAGCAGTAAG-3′; Dkk-4R, 5′-AAAAATGGCGAGCACAGC-3′; Axin2F, 5′-GAGAGTGAGCGGCAGAGC-3′; Axin2R, 5′-CGGCTGACTCGTTCTCCT-3′; Fzd7F, 5′-GGGTATCTCTGTGTAGCCCTGA-3′; Fzd7R, 5′-AGAGGCAGGTGGATGTCTGT-3′; Pgk1F, 5′-TACCTGCTGGCTGGATGG-3′; Pgk1R, 5′-CACAGCCTCGGCATATTTCT-3′; HIF-1α KOF, 5′-GCACTAGACAAAGTTCACCTGAGA-3′, HIF-1α KOR, 5′ CGCTATCCACATCAAAGCAA-3′.

ChIP primers used were as follows: Lef-1 P1F, 5′-TTCCCAGCGCTCATCATCA-3′;

Lef-1 P1R, 5′-CCTTTCGCTTCGGTTTTCCT-3′; Lef-1 P2F, 5′-AAAACAAAACCCCAAATCACC-3′; Lef-1 P2R, 5′-TCACCGTGCAAAACCTCTC-3′; Lef-1 P3F, 5′-CGGCGTAGACGCTCTCAG-3′; Lef-1 P3R, 5′-CGCTTTCCCACTTAGAAGGAC-3′; Tcf-1 P1F, 5′-ACACCGAAACGTTCTTGAGGC-3′; Tcf-1 P1R, 5′-TCACCACGACCGATCACTGTT-3′; Tcf-1 P2F, 5′-GGATGCAACTTCCCAGACTGAG 3′; Tcf-1 P2R, 5′-GCTTAGAACCTGCTGTCCAGGA-3′.

Immunoprecipitation assay. For chromatin immunoprecipitation (ChIP) experiments, the sonicated nuclear extracts of hypoxic cells were immunoprecipitated with anti-HIF-1α monoclonal antibody (Novus Biologicals), reverse cross-linked and analysed by qRT–PCR. For immunoprecipitation experiments, 500 μg of hypoxic ES nuclear protein extracts were cleared with either 10 μl of anti-HIF-1α polyclonal antibody (Novus Biologicals) pre-coupled to protein-G-sepharose (Roche), or 5–10 μl of anti-LEF-1 polyclonal antibody (Cell Signaling) pre-coupled to protein-A sepharose (Roche).

Generation and analysis of mice. Generation and analysis of *Hif-1α*$^{f/f}$ (ref. 19), *CamKIIalpha-Cre*[20], and *Ubc–Cre–ER*^{T2} (ref. 32) has been described previously. *BAT–GAL* reporter mice were obtained from the Jackson laboratory and genotyped as described previously[17]. To generate global *Hif-1α*$^{Δ/Δ}$ knockout mice (g*Hif-1α*$^{Δ/Δ}$), *Hif-1α*$^{f/f}$ mice were crossed with *Hif-1α*$^{f/f}$ mice expressing *Ubc–Cre–ER*^{T2} and offspring were screened for the presence of *1lox P* using the genotyping primers P1: 5′-GCAGTTAAGAGCACTAGTTG-3′, P2: 5′-GGAGCTATCTCTCTAGACC-3′ and P3: 5′-TTGGGGATGAAAACATCTGC-3′. Cre mediated recombination between the *loxP* sites in the *2loxP* allele produces the *1loxP* allele, which lacks exon 2 and results in a mutant mRNA transcript containing multiple in frame stop codon downstream of exon 1 sequences. Tamoxifen free base (MP Biomedicals) was administered to nursing mothers at a concentration of 200 mg kg^{-1}, as described previously[33], to induce recombination. Neuronal deletion of *Hif-1α*$^{f/f}$ (*nHif-1α*$^{Δ/Δ}$) was achieved by crossing mice carrying *Hif-1α*$^{f/f}$ alleles with *Hif-1α*$^{f/f}$ mice expressing Cre recombinase under the control of the calcium/calmodulin-dependent kinase Cam KIIα promoter (CamKII–Cre) as described previously[21]. All mice were maintained in micro-isolator cages and treated in accordance with NIH and American Association of Laboratory Animal Care Standards, and consistent with the animal care and use regulations of the University of Pennsylvania, Philadelphia.

LacZ and hypoxyprobe detection. Dissected embryos, or sections from adult organs were washed in PBS, fixed for 30 min in 4% paraformaldehyde, and incubated in the 5-bromo-4-chloro-3-indolyl-β-d-galactosidase (X-Gal) staining solution for 0.5–16 h. Hypoxic regions in developing mouse embryos and adults were detected using pimonidazole hydrochloride detection kit (Chemicon), according to the manufacturer's protocol. Briefly, pimonidazole in water was administered intraperitoneally at a dosage of 60 mg kg^{-1}. To minimize hypoxyprobe background, a washout period of 1 h was allowed. Animals were killed and brains were removed following cardiac perfusion.

Antibodies for immunoblotting, immunofluorescence and quantitation. Western blot analysis was performed using the following primary antibodies: Lef 1, Tcf-1, HIF-1α, CREB, GSK 3β, pGSK 3β (Cell signaling Technologies) and β catenin (BD Transduction Laboratories) at 1:1000 dilution, ARNT (Cell Signalling Technologies) at 1:500 dilution and actin (Cell Signalling Technologies) at 1:10,000 dilution for 10 h at 4 °C. Secondary antibodies were used at 1:300 dilution for 1 h at room temperature. Staining for immunochemistry was carried out using the following primary antibody dilutions: β-tubulin III, Nestin and Doublecortin (Abcam) at 1:1,000, HIF-1α (Cayman) at 1:200, Laminin (Sigma) at 1:50, Cre recombinase monoclonal (Covance), and Sox2 (Chemicon and R&D Systems) at 1:500 for 10 h at 4 °C, BrdU (USBiologicals) at 1:1,000 in PBS, and β-galactosidase polyclonal (Fitzgerald) at 1:100 for 12 h at room temperature. Hypoxyprobe (Chemicon) was used at 1:500 dilution for 1 h at room temperature. Fluorescent conjugated secondary antibodies were used at a 1:400 dilution for 1 h at room temperature.

To examine the effects of *Hif-1α* deletion, young adult (7–8 weeks) neuronal or global *Hif-1α*$^{Δ/Δ}$, or control mice lacking Cre (*Hif-1α*$^{f/f}$), were injected with BrdU (5-bromo-2′-deoxyuridine, 100 mg kg^{-1}, for four consecutive days) (Roche) to label proliferating AHPs and their progeny. Mice were perfused after the final BrdU injection. For rescue analysis of neuronal defects, animals were injected with either GSK3 inhibitor SB216763 (2 mg kg^{-1}), or vehicle (DMSO) every alternate day for 7 doses, as described previously[34]. For tissue staining, organs were removed from perfused experimental animals and embedded in Tissue Tek optimal cutting temperature (OCT) medium (Fisher), then frozen to –80°C for storage. Frozen sections (14 μm) were cut using a Microm HM 550 cryostat. Sections were fixed with 5% buffered formalin for 2 min, washed three times in PBS and incubated in protein blocking agent for 30 min at room temperature. Primary antibody cocktails of BrdU and DCX diluted in 2% BSA in PBS, or according to the manufacturer's protocol, were then added to the tissue sections and incubated at 4°C overnight. Slides were washed three times in PBS and then incubated in secondary antibody cocktail in 3% BSA in PBS for 1 h. Slides were mounted in Vectashield mounting medium (Vector Laboratories) and visualized on a Leica Leitz 500 microscope. Images were acquired and processed using Photoshop CS3 (Adobe).

For quantification of BrdU$^+$, DCX$^+$ and β-galactosidase$^+$ cells, and for the enumeration of laminin-positive vessels, 5–7 tissue sections offering an anterior to posterior coverage of the dentate gyrus from each animal were stained. Positive cells were counted per field (at ×10 magnifications) and correlated per mice. The

© 2010 Macmillan Publishers Limited. All rights reserved.

results were pooled to generate mean values. For neurite quantification, DCX^+ cells with processes longer than 20 μm extensions were counted as positive.

Neural stem cell isolation, culture, differentiation and transfection. Mouse ventral mesencephalon E14 neurospheres were purchased from STEMCELL Technologies. Isolated neural stem cells and embryonic neurospheres (STEMCELL Technologies) were cultured using the STEMCELL Technologies kit (05715). Briefly, 5–6 hippocampi dissected from 4–6 week young adult mice were collected in a dish containing neurocult tissue collection solution. The tissue was chopped into small pieces using a razor, subjected to brief enzymatic dissociation in Neurocult dissociation solution at 37°C, mechanically dissociated by gentle pipetting, and resuspended in Neurocult resuspension solution. Primary cells were seeded at a density of 1×10^5 cells in T-25cm^2 flasks, and growth of neursopheres monitored under the microscope. For transfection, cultures of 3–4 day-old neurospheres generated from a seeding density of 2×10^6 cells 10 ml^{-1} were diluted 1:3, plated into 24 or 6-well dish (0.5–3 ml) and transfected with 0.5–2 μg plasmid using Lipofectamine 2000 (Invitrogen). Samples were analysed for mRNA or reporter activity 48 h after transfection. For differentiation assay, neurospheres were seeded on poly-ornithine-coated glass coverslips and cultured in Neurocult differentiation media (STEMCELL Technologies). For immunostaining of neurospheres, the floating spheres were first attached to glass coverslips using Cell-Tak cell tissue adhesive (BD) and then processed similarly to adherent cells.

Generation of ES-*lef-1* cells. *Lef-1* cDNA (OpenBiosystems: MMM1013-9334706) was subcloned into pLKO.1 neo (Addgene: Plasmid 13425, provided by S. Stewart, Washington University, USA) with *Age*1 and *Eco*R1. LEF-1-overexpressing lentivirus was prepared in HEK293T cells using the pMDLg/pRRE, pRSV-Rev and envelope system. ES cells were transduced with virus supernatant and selected with 0.4 mg ml^{-1} geneticin. ES cells transduced with empty pLKO.1 neo virus (VC) served as control.

Generation of SA-β-catenin lentivirus and stereotactic injection. The control vector was pHIV-IRES-Zsgreen (Addgene: Plasmid 18983, provided by Z. Werb and B. Welm, UCSF, USA). ΔGSK β-catenin insert has been described before[22]. The insert was subcloned into pHIV-IRES-Zsgreen. High-titre lentivirus (~2×10^9 transducing units ml^{-1}, 1 μl) was injected bilaterally into the dentate gyrus of 10–12 week-old mice (AP -2, ML ±1.5, DV −1.8 from Bregma, $n = 3$–5 per group) as described previously[34]. Viral spread was assessed by visualizing the presence of Zsgreen-positive cells along the anterior–posterior axis of the dentate gyrus (about 1.2–1.6 mm). Following 2 weeks of recovery, mice were injected intraperitoneally with BrdU (100 mg kg^{-1}) daily for 4 days. The mice were then perfused with 4% paraformaldehyde and hippocampal sections processed for BrdU and DCX staining.

Statistical analyses. Statistical significance was computed using Student's *t*-test or one-way ANOVA, and significance was set at $P < 0.05$.

30. Maltepe, E., Schmidt, J. V., Baunoch, D., Bradfield, C. A. & Simon, M. C. Abnormal angiogenesis and responses to glucose and oxygen deprivation in mice lacking the protein ARNT. *Nature* **386,** 403–407 (1997).
31. Maltepe, E., Keith, B., Arsham, A. M., Brorson, J. R. & Simon, M. C. The role of ARNT2 in tumor angiogenesis and the neural response to hypoxia. *Biochem. Biophys. Res. Commun.* **273,** 231–238 (2000).
32. Ruzankina, Y. *et al.* Deletion of the developmentally essential gene ATR in adult mice leads to age-related phenotypes and stem cell loss. *Cell Stem Cell* **1,** 113–126 (2007).
33. Gruber, M. *et al.* Acute postnatal ablation of Hif-2α results in anemia. *Proc. Natl Acad. Sci. USA* **104,** 2301–2306 (2007).
34. Mao, Y. *et al.* Disrupted in schizophrenia 1 regulates neuronal progenitor proliferation via modulation of GSK3β/β-catenin signaling. *Cell* **136,** 1017–1031 (2009).

© 2010 Macmillan Publishers Limited. All rights reserved.

nature cell biology

DOI: 10.1038/ncb2102

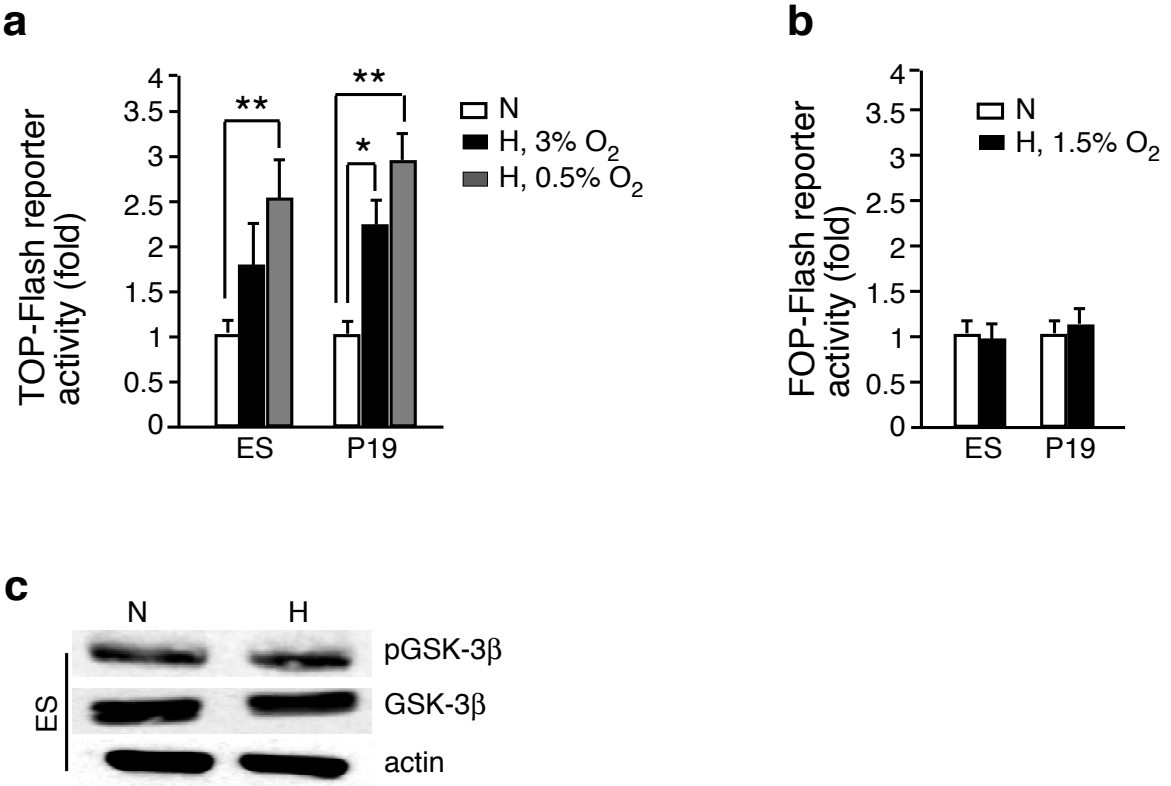

Figure S1 Hypoxia activates Wnt/β-catenin signalling in embryonic cells. **a**, ES and P19 EC cells transiently transfected with TOP-Flash reporter plasmid were cultured under different low O_2 levels (0.5% and 3%) for 16 h (n=6). **b**, No significant enhancement of FOP-Flash reporter activity was observed in hypoxic cells (1.5% O_2 or other low O_2 levels [data not shown]) over cells cultured under normoxia (n=6). Luciferase activity from pRL-SV40 reporter co-transfected with TOP-Flash or FOP-Flash reporter plasmids was used for normalization. **c**, Western blot analysis of whole cell extracts of ES cells cultured under normoxia or hypoxia for phosphorylated GSK-3β, and total GSK-3β. Actin served as the loading control. *= P <0.05, **= P <0.005., Student's t-test. Error bars represent S.D.

© 2010 Macmillan Publishers Limited. All rights reserved.

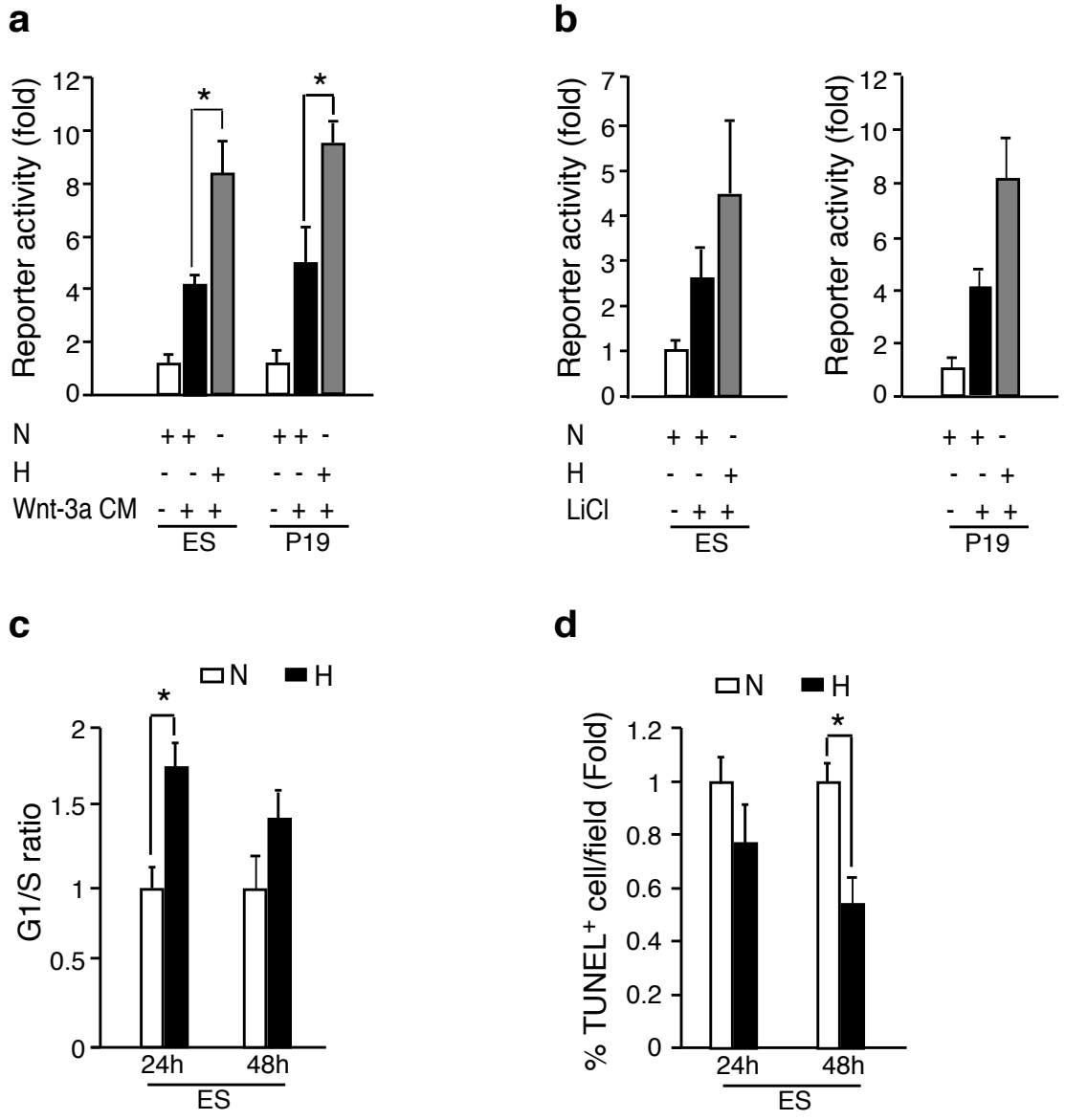

Figure S2 Hypoxia increases Wnt/β-catenin activity in stimulated cells. **a**, **b**, TOP-Flash reporter activity in ES and P19 EC cells treated with either Wnt-3a CM or LiCl and cultured either under 21% or 1.5% O_2 for 16 h (n=9). Whereas Wnt-3a CM and LiCl stimulates TOP-Flash activity, exposure to 1.5% O_2 further increases TOP-Flash activity in stimulated cells. **c,** Cell-cycle analyses for ES cells after exposure to normoxia or hypoxia (1.5% O_2) for 24 h or 48 h. Cells were labelled with BrdU, stained with propidium iodide (PI) and analysed by flow cytometry (n=3 independent experiments). Increased G1/S ratio of hypoxic ES cells indicates increased accumulation in G1 stage, and delayed S-phase entry. Note G1/S phase ratio decreases in ES cells exposed to hypoxia for 48h, as compared to cells cultured under hypoxia for 24 h. **d**, Decreased cell death in ES cells cultured under hypoxia as compared to normoxic control cells (n=3 plates, 9 random fields in each plate) assessed by a TdT mediated dUTP nick end labelling (TUNEL) assay. Increased cell survival likely accounts for ES cell expansion under prolonged hypoxia (Fig. 1g). *= P<0.05., Student's t-test. Error bars represent S.D.

© 2010 Macmillan Publishers Limited. All rights reserved.

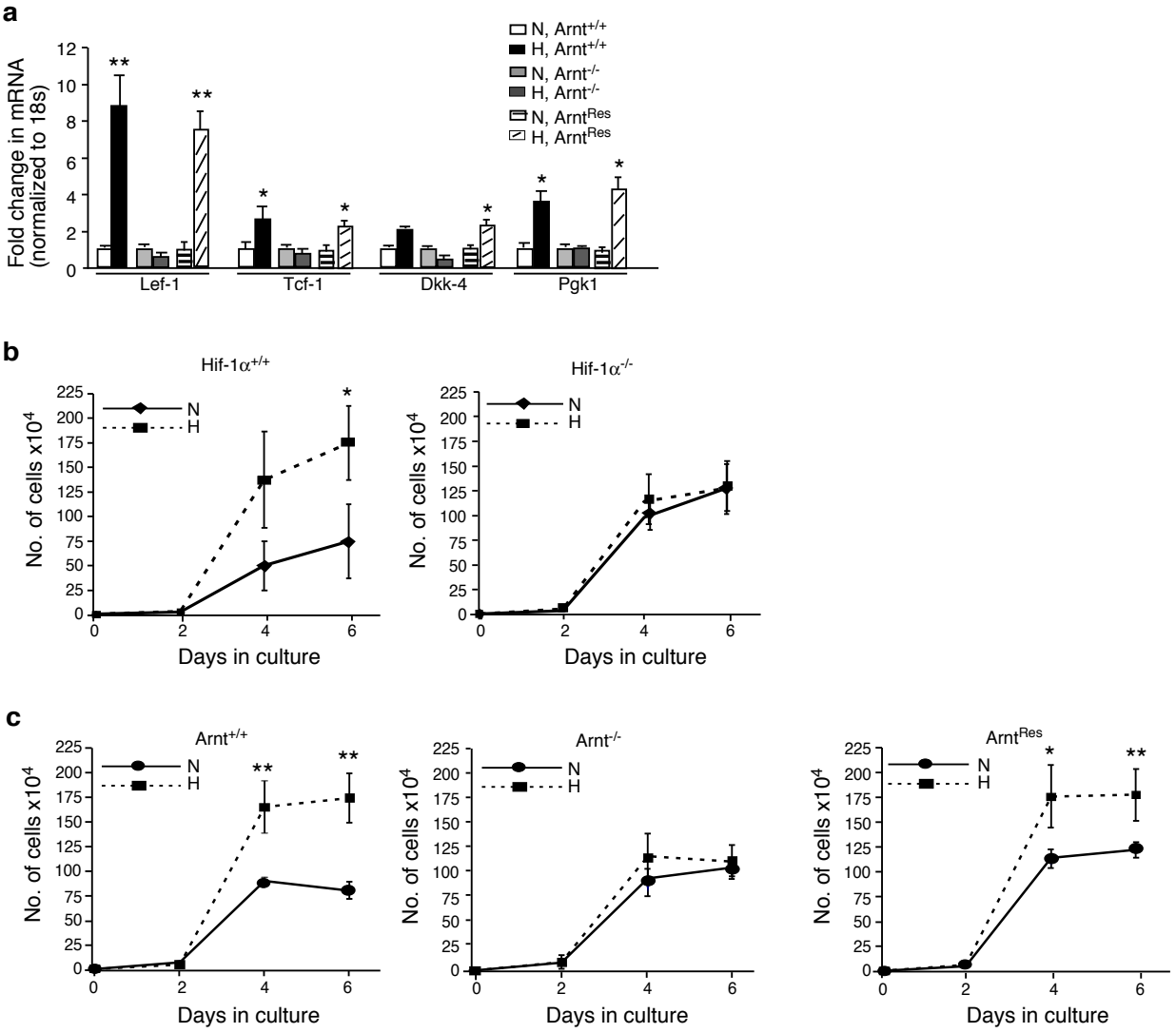

Figure S3 HIF-1α and ARNT are required for hypoxic activation of Wnt/β-catenin signalling in embryonic cells. **a,** qRT-PCR analysis of Wnt-3a target genes in *Arnt* $^{+/+}$, *Arnt* $^{-/-}$ and *Arnt* ^{Res} ES cells show direct dependence of Wnt induction on hypoxic ARNT activity (n=3). **b, c,** Cells were plated at a density of 10^4 cells per 60 mm^2 and cultured under normoxia or 1.5% O_2 for 6 days. Numbers were assessed by cell counts in a hemocytometer at indicated time points. *Hif-1α* $^{+/+}$(**b**), *Arnt* $^{+/+}$ and *Arnt* ^{Res} (**c**) cells displayed cell number expansion under hypoxia. To the contrary, hypoxic *Hif-1α* $^{-/-}$ (**b**) and *Arnt* $^{-/-}$ (**c**) cells grew at rates comparable to normoxic control cells. *= P <0.05, **= P <0.005., Student's t-test. Error bars represent S.D.

© 2010 Macmillan Publishers Limited. All rights reserved.

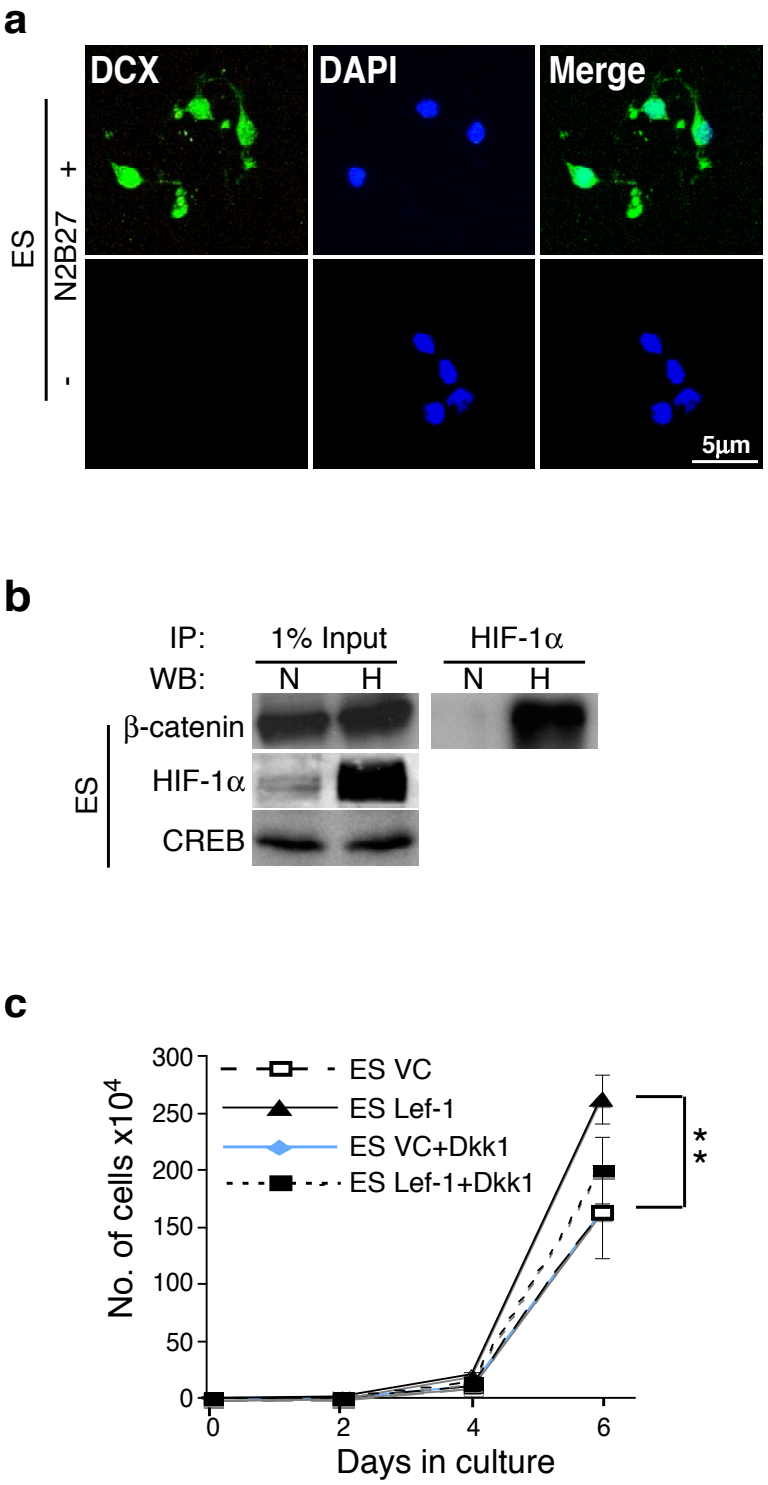

Figure S4 ES cell differentiation, HIF-1α/β-catenin interaction and LEF-1 modulation of ES cell growth. **a**, ES cells treated with (+) or without (-) N2B27 neuronal growth and differentiation supplements differentiate into neurons as indicated by the expression of the neuronal marker doublecortin (DCX) in green. The nuclei are stained with DAPI (blue). **b**, Immunoprecipitation with HIF-1α antibody was performed on nuclear extracts of normoxic or hypoxic (1.5% for 20 h) ES cells. CREB served as the loading control. **c,** ES-*Lef-1* cells were plated at a density of 10^4 cells per 60 mm^2, cultured under normoxia and cell numbers assessed over 6 days. Empty virus transduced (VC) cells served as control. Both cell lines were also treated with DKK-1 (300 ng ml^{-1}). **= P <0.005., Student's *t*-test. Error bars represent S.D.

© 2010 Macmillan Publishers Limited. All rights reserved.

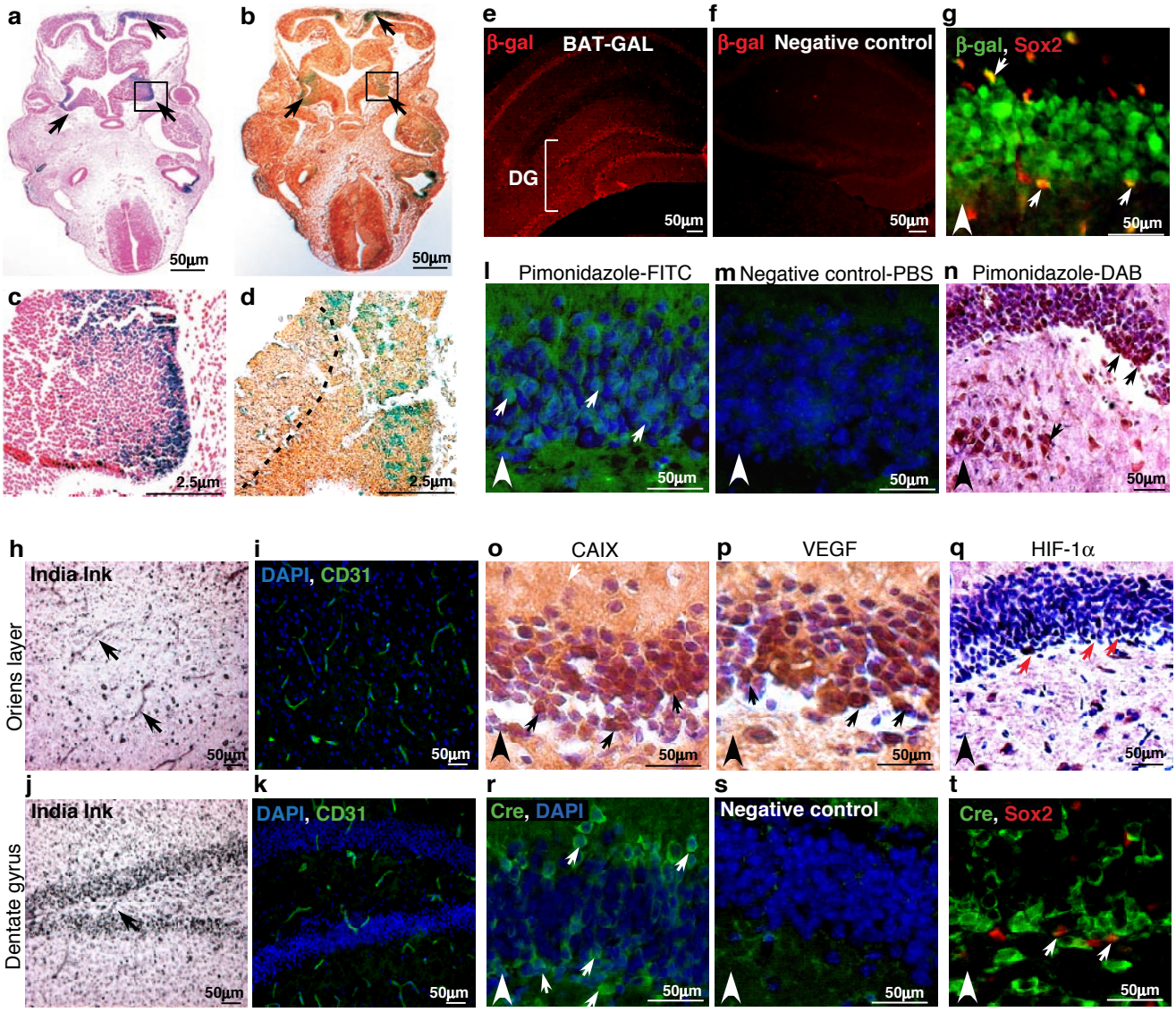

Figure S5 Hypoxic regions in embryonic and adult brain. **a, b,** Wnt /β-catenin activity marked by β-galactosidase enzyme staining (blue) in E11.5 *BAT-GAL* reporter mice (**a**) is closely associated with hypoxic regions marked by pimonidazole staining (brown) in an adjacent β-galactosidase enzyme stained (blue) embryonic section (**b**). (**c, d**) Magnifications of the boxed region in (**a**) and (**b**). Black line in (**d**) demarcates highly hypoxic region from the adjacent light brown area. **e-g**, β-galactosidase (β-gal) immunostaining in *BAT-GAL* reporter line (**e**) and wildtype control (**f**) identifies the GCL as active for Wnt/β-catenin signalling. **g**, Co-expression of β-galactosidase and Sox2 in neural stem cells in the SGZ. **h-k**, India black ink and CD31 mark fewer blood vessels in the GCL of the DG (**j, k**) as compared to the Oriens layer of the hippocampus (**h, i**). **l-n**, Pimonidazole immunofluorescence staining (**l**) and enzymatic immunodetection (**n**) indicates the presence of hypoxic pockets in the GCL. The hippocampus of PBS injected animals served as a negative control (**m**). **o-q**, Expression of CAIX (**o**), VEGF (**p**) and stabilization of nuclear HIF-1α (**q**) within the GCL of the DG. **r-t**, Nuclear (arrows) and cytoplasmic distribution of Cre in the GCL of αCamKII-Cre R1 line (**r**). Cre negative mice served as a negative control (**s**). Colocalization with $Sox2^+$ cells (arrows) indicates the expression of Cre in neural stem and progenitor cells in the SGZ (**t**). In **e-t**, arrowheads point towards the SGZ, and arrows indicate the relevant cells.

© 2010 Macmillan Publishers Limited. All rights reserved.

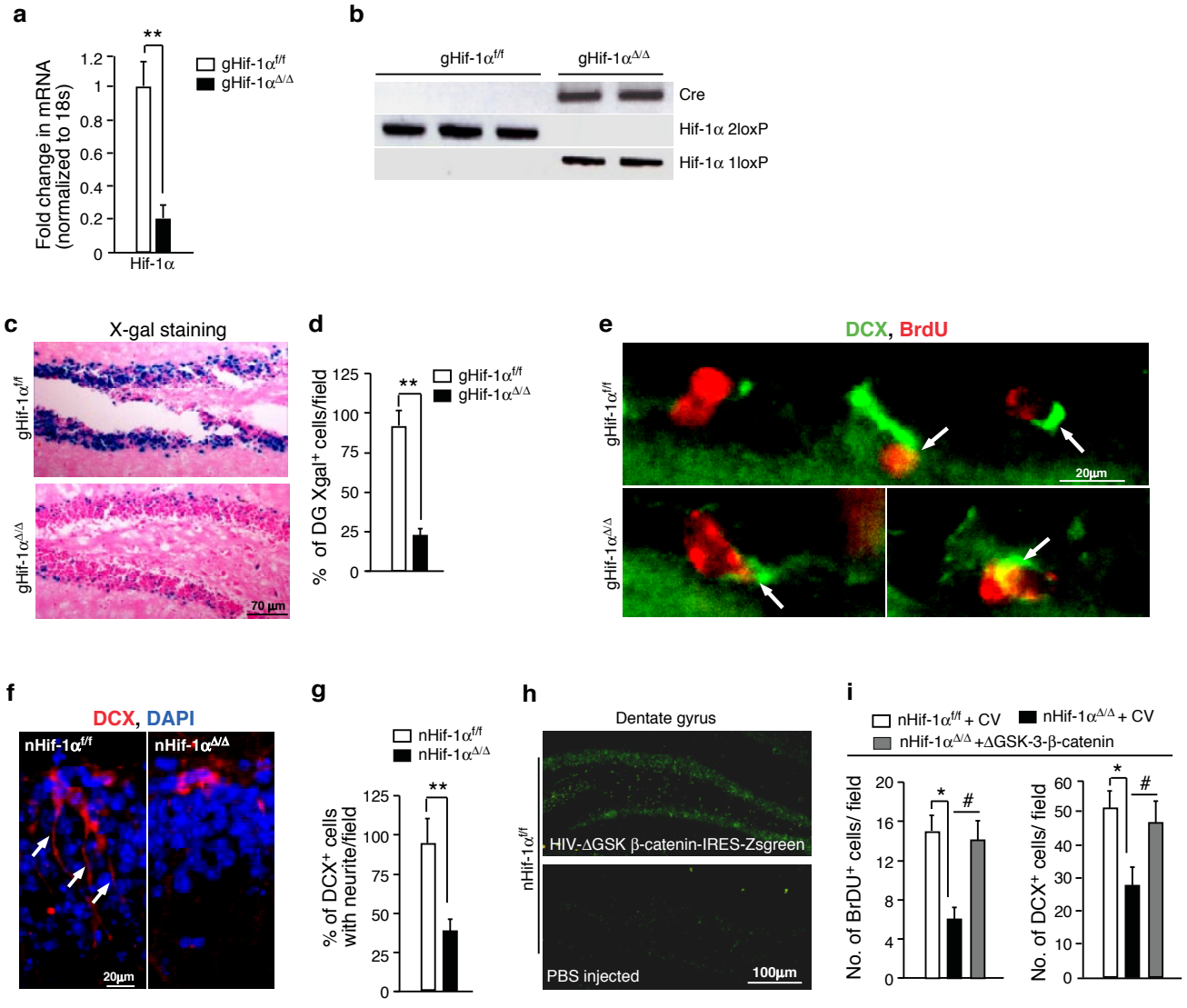

Figure S6 *In vivo* deletion of *Hif-1α* impairs adult hippocampal neurogenesis and Wnt/β-catenin signalling. **a**, qRT-PCR confirmation of *Hif-1α* deletion in the adult hippocampal extracts of *gHif-1α*$^{\Delta/\Delta}$ mice (*n=3-4* in each group). **b**, PCR genotyping indicating *Cre* mediated deletion of *Hif-1α* marked by the absence of *2loxP* band and the presence of *Cre* and *1loxP* bands (*gHif-1α*$^{\Delta/\Delta}$ mice). The recombination efficiency of Cre is variable. Weak *2loxP* band was detected in some *Hif-1α*$^{\Delta/\Delta}$ mice (data not shown). **c**, β-galactosidase enzyme (X-gal) staining of the dentate gyrus of *Hif-1α*$^{f/f}$, *BAT-GAL*^{Tg} (c upper panel) and *gHif-1α*$^{\Delta/\Delta}$, *BAT-GAL*^{Tg} (c lower panel). **d**, 4 fold reduction in Wnt activity as assessed by X-gal staining in the dentate gyrus of adult *gHif-1α*$^{\Delta/\Delta}$ compared to *gHif-1α*$^{f/f}$ control animals (*n=3,* 5 sections per animal). **e**, DCX (green) and BrdU (red) double positive cells (white arrows) reveal post-mitotic neurons in the SGZ and GCL of *gHif-1α*$^{f/f}$ (upper) and *gHif-1α*$^{\Delta/\Delta}$ mice (lower). **f**, **g**, *In vivo* deletion of neuronal Hif-1α impairs adult hippocampal neuronal morphology (n=*3*). *= *P* <0.05, **= *P* <0.005., Student's *t*-test. Error bars represent S.E.M.. **h**, Stereotactic injection of Δ-GSK3-β-catenin lentivirus (HIV- ΔGSK3-β-catenin-IRES-Zsgreen) into the adult DG (12-16 weeks) is detected by green fluorescence, which is absent in PBS injected adult DG. **i,** Quantification of BrdU$^+$ (i left panel) and DCX$^+$ (i right panel) cells in *nHif-1α*$^{\Delta/\Delta}$ DG transduced with high titer Δ-GSK3-β-catenin lentivirus. Following 2 weeks of recovery, mice were injected with BrdU (100 mg Kg^{-1}) i.p daily for 4 days. Control virus treated *nHif-1α*$^{\Delta/\Delta}$ and *nHif-1α*$^{f/f}$ mice served as controls (*n=3-5* per group). Statistical significance (**i**) was computed using one-way ANOVA. *nHif-1α*$^{\Delta/\Delta}$ animals transduced with high titer Δ-GSK3-β-catenin lentivirus displayed remarkable increase in BrdU$^+$ and DCX$^+$ cell counts as compared to control virus treated *nHif-1α*$^{\Delta/\Delta}$ animals, and is approaching significance (# indicates *P*=0.06). Error bars represent S.E.M.

© 2010 Macmillan Publishers Limited. All rights reserved.

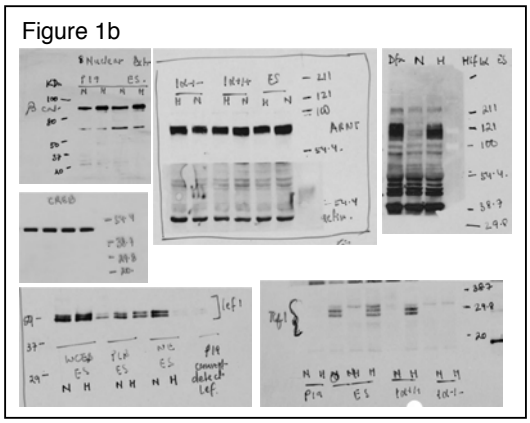

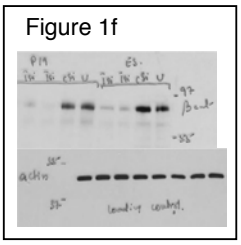

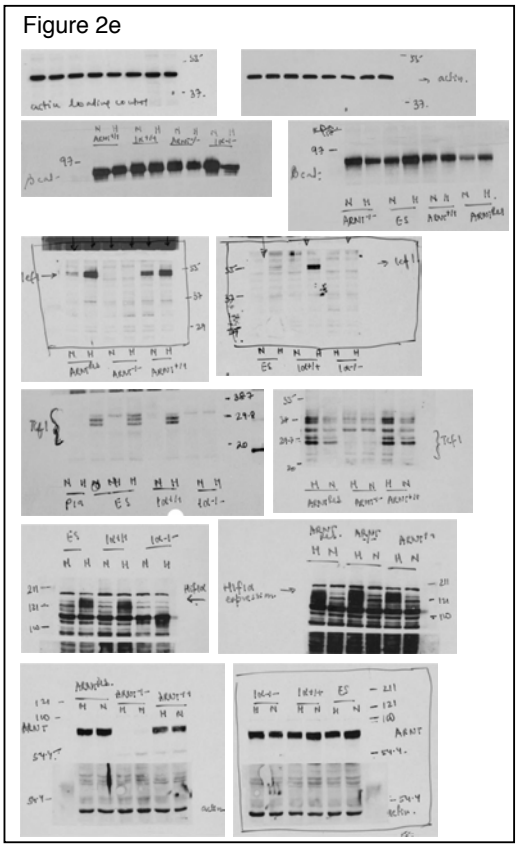

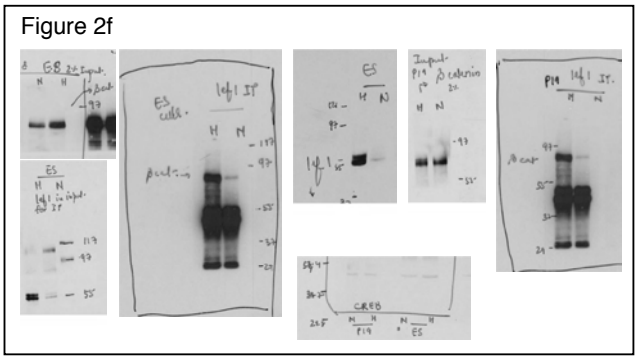

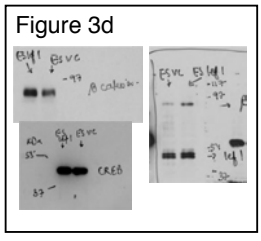

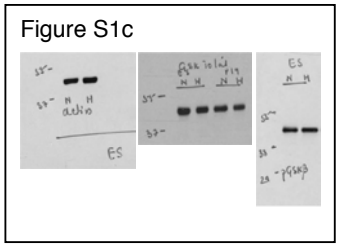

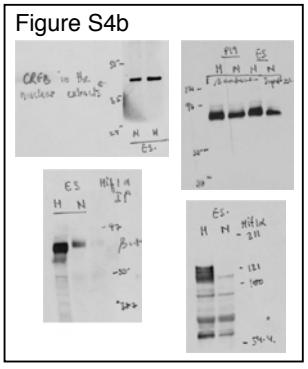

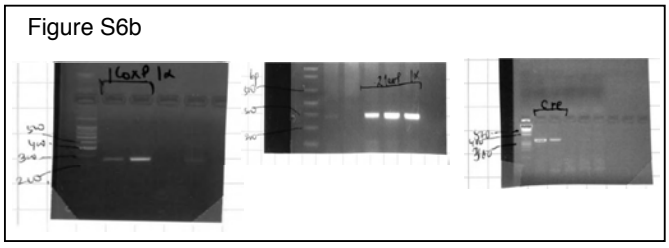

Figure S7 Uncropped blots

© 2010 **Macmillan Publishers Limited. All rights reserved.**